

See discussions, stats, and author profiles for this publication at: <https://www.researchgate.net/publication/242330595>

Electrogenerated Conductive Polymers from Triphenylamine End-Capped Dendrimers

ARTICLE *in* MACROMOLECULES · JUNE 2013

Impact Factor: 5.8 · DOI: 10.1021/ma401085q

CITATIONS

10

READS

77

8 AUTHORS, INCLUDING:



[Rolando A. Spanevello](#)

Rosario National University

74 PUBLICATIONS 578 CITATIONS

[SEE PROFILE](#)



[Daniel A. Heredia](#)

Instituto de Química Rosario

7 PUBLICATIONS 116 CITATIONS

[SEE PROFILE](#)



[Gabriela Marzari](#)

Centro de Investigaciones en Química Biológi...

7 PUBLICATIONS 103 CITATIONS

[SEE PROFILE](#)



[Fernando Fungo](#)

Universidad Nacional de Río Cuarto

35 PUBLICATIONS 865 CITATIONS

[SEE PROFILE](#)

Electrogenerated Conductive Polymers from Triphenylamine End-Capped Dendrimers

María I. Mangione and Rolando A. Spanevello*

Instituto de Química Rosario, Facultad de Ciencias Bioquímicas y Farmacéuticas, Universidad Nacional de Rosario—CONICET, Suipacha 531, S2002RLK Rosario, Argentina

Angel Rumbero

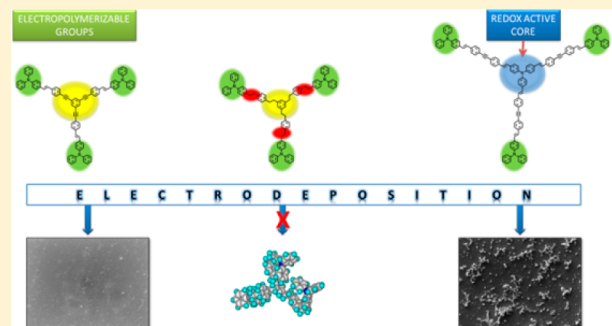
Departamento de Química Orgánica, Facultad de Ciencias, Universidad Autónoma de Madrid, Cantoblanco, 28049 Madrid, Spain

Daniel Heredia, Gabriela Marzari, Luciana Fernandez, Luis Otero, and Fernando Fungo*

Departamento de Química, Universidad Nacional de Río Cuarto, Agencia Postal 3 (X5804BYA), Río Cuarto, Argentina

Supporting Information

ABSTRACT: Electroactive end-capped dendritic macromolecules were designed and synthesized. Their structures contain triphenylamine moieties as part of the core or dendrons. The electro-generated films produced with these monomers behaved as conductive dendritic polymers that can be reversible charged, both in the core and in the peripheral units. The design of dendrimer structures with the introduction of systematic changes allows to establish relationships between their electro-optical properties with molecular structural parameters. The films of polymeric material hold good electrical conductivity, reversible electrochemical processes and chemical stability. The results indicate that the use of conjugated and rigid structures in dendritic macromolecules is an important factor in order to obtain electropolymeric films. This work provides a model to design starburst dendrimers capable to form electrochemically active polymers with potential applications in electronic and optoelectronic devices.



INTRODUCTION

The development of organic materials with application in molecular organic electronics, nanotechnology, and optoelectronic devices (like organic solar cells and organic light emitting diodes, OLEDs) have shown a remarkable scientific activity due to the relevance of these technologies in the generation and rational use of energy.^{1–3} Optoelectronic devices are optical-to-electrical transducers that can produce photoinduced charge separated states, and/or light by charge recombination. Using organic materials as optoelectronic devices is a challenging target, because these materials must be designed in order to include efficient light absorption-emission capability, correct work function, appropriate electron and hole transporting characteristics, malleability, adequate solid properties and chemical stability. Two key factors in devices operation are hole–electron transporting, and their injection through the heterogeneous interfaces in the contact electrodes. In most multiple layers optoelectronic devices, the hole transporting layer (HTL) and the electron transporting layer (ETL) control the charge balance and the injection-collection into/from them.⁴

One of the materials used as hole transporting layer with more recent development are dendrimers. These molecules, with highly branched three-dimensional architecture, present multiple chains emanating from a single core.^{5,6} Dendrimers are monodispersed macromolecules possessing well-defined structures, that can be precisely tailored with discrete functionalities to create multifunctional materials. Their unique structures and properties make these macromolecules suitable subjects for a wide range of biomedical and industrial applications, such as drug delivery,⁷ multivalent bioconjugate and multivalent diagnostics for magnetic resonance imaging (MRI),⁸ extremely efficient light-harvesting antenna,⁹ and homogeneous catalysis.¹⁰ Recently, dendrimers have also found promising applications as materials for organic electronic devices, such as photoactive and electroactive materials in OLEDs,^{11–16} solar cells,^{17–19} and transistors.^{20,21} Reported advantages of some starburst molecules are the good charge transporting properties, and low energy barrier for hole injection to the anode with

Received: May 24, 2013

Revised: May 27, 2013

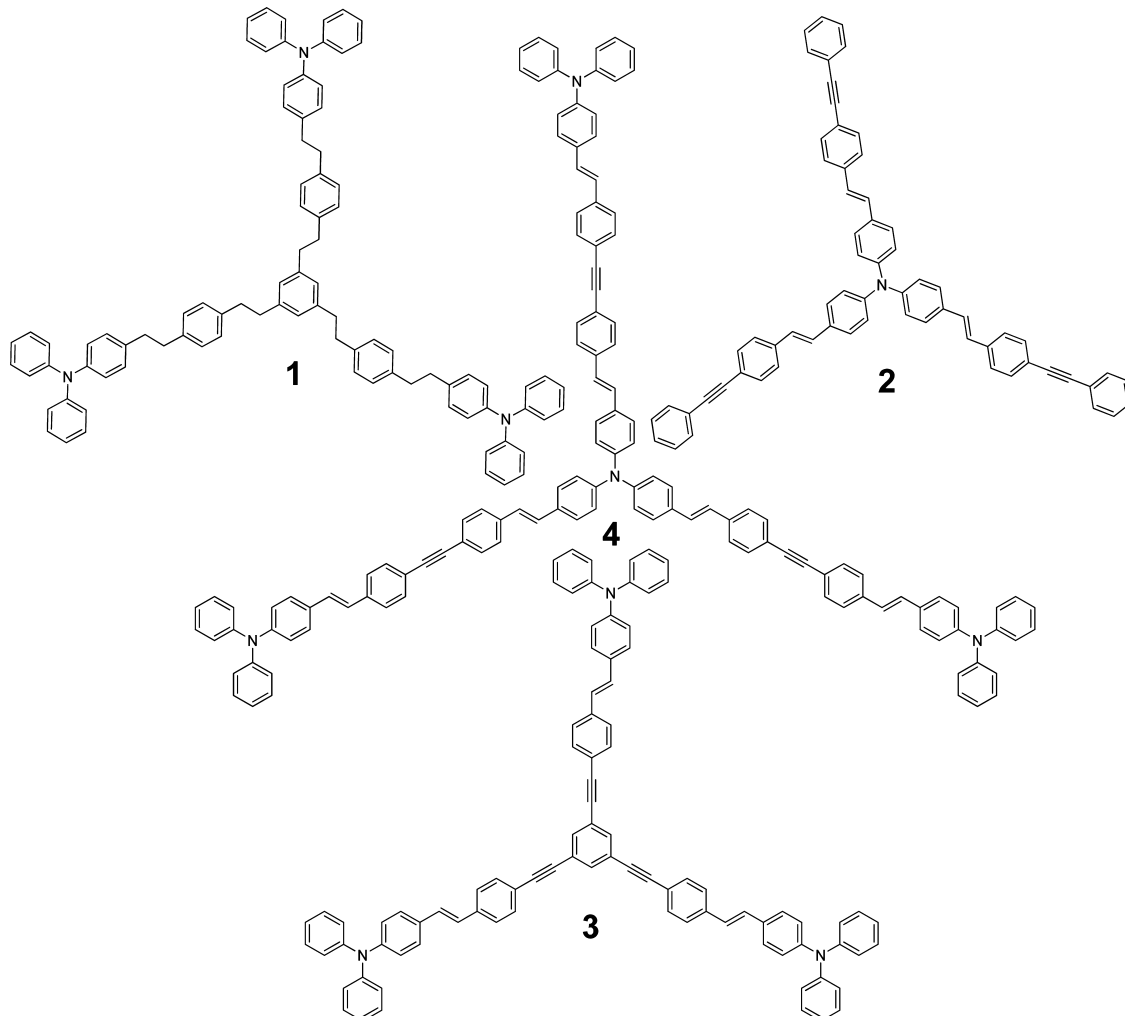


Figure 1. Dendrimer structures.

electron block injection capability.^{14,20} In addition, these macromolecules have a high glass-transition temperature (T_g), which is a very important factor in order to avoid device degradation by the morphological changes produced by Joule effect during operation.^{22–26} Moreover, the branched three-dimensional architecture nature of dendrimeric material is also convenient to retain optoelectronic properties in solid state devices, due to the fact that they can avoid aggregation effects.

This type of devices also demands materials with capability for thin films formation using low cost technologies. The most used methods to deposit organic material for optoelectronic devices are thermal evaporation and solution-processing (drop casting, spin coating, etc.). Although thermal evaporation with the use of fine mask can produce well-patterned films, the process is slow and demands expensive vacuum equipment. In addition, thermal evaporation requires materials with high sublimation capability and excellent thermal stability, which are properties not easily obtained in polymers. Also, low-cost solution processes, such as spin-coating and deep-coating, widely used in the production of nonpatterned films, require material with intrinsic high solubility, and usually produce large amount of waste. An alternative important technique to produce conducting films is the electropolymerization. The deposition of organic material over a conducting substrate through electrochemical polymerization is a versatile method

that allows synthesizing a conducting film in one step.^{27,28} The technique permits to obtain films with different forms and patterns, with easy control in the thickness.^{28–32} A number of reports revealed that the polymeric films obtained electrochemically over conductive solid substrates are highly stable, with excellent adherence to the electrode. These materials often hold high charge transporting capability and considerable fluorescence properties in some special cases.^{28–33} Additionally, we have demonstrated that by controlling the electrodeposition conditions, it is possible to optimize the morphology of the surface, and consequently the film optoelectronic properties.²⁷

In this article, we report the synthesis and properties of functional starburst monomers featuring the presence or absence of electroactive central core connected by conjugated branches to peripherals triphenylamine (TPA) moieties (Figure 1). The introduction of systematic changes in the design of dendrimer structures allows to establish relationships between their electro-optical properties with molecular structural parameters. These new electropolymerizable macromolecules exhibit interesting electronic properties that yield thin films of polymeric material with good electrical conductivity, reversible electrochemical processes and stability. Hence, this work provides a model for designing starburst dendrimers capable to form electrochemically active polymers with potential applications in electronic and optoelectronic devices.

■ EXPERIMENTAL SECTION

Instrumentation and Characterization Techniques. Melting points were taken on a Leitz Wetzlar Microscope Heating Stage, Model 350 apparatus and are uncorrected. ¹H and ¹³C NMR spectra were recorded on Bruker Avance-300 spectrometer with Me₄Si as the internal standard and chloroform-d as solvent. Abbreviations: s = singlet, d = doublet, t = triplet, and m = multiplet expected but not resolved. Mass spectra of dendrons were recorded in a Shimadzu QP2010 Plus instrument, ion source temperature = 300 °C, and detector voltage = 70 kV. Samples were analyzed by ultraviolet matrix assisted laser desorption-ionization mass spectrometry (UV-MALDI MS) and by ultraviolet laser desorption-ionization mass spectrometry (UV-LDI MS) performed on the Bruker Ultraflex Daltonics TOF/TOF mass spectrometer (Leipzig, Germany). Mass spectra were acquired in linear positive and negative ion modes. Stock solutions of samples were prepared in chloroform. External mass calibration was made using β -cyclodextrin (MW 1134) with nHo as matrix in positive and negative ion mode. Sample solutions were spotted on a MTP 384 target plate polished steel from Bruker Daltonics (Leipzig, Germany). For UV-MALDI MS matrix solution was prepared by dissolving GA (gentisic acid, 1 mg/mL) in water and dry droplet sample preparation was used according to Nonami et al.³⁴ loading successively 0.5 μ L of matrix solution, analyte solution and matrix solution after drying each layer at normal atmosphere and room temperature. For UV-LDI MS experiments two portions of analyte solution (0.5 μ L \times 2) were loaded on the probe and dried successively (two dry layers). Desorption/Ionization was obtained by using the frequency-tripled Nd:YAG laser (355-nm). The laser power was adjusted to obtain high signal-to-noise ratio (S/N) while ensuring minimal fragmentation of the parent ions and each mass spectrum was generated by averaging 100 lasers pulses per spot. Spectra were obtained and analyzed with the programs FlexControl and FlexAnalysis, respectively. Reactions were monitored by TLC on 0.25 mm E. Merck Silica Gel Plates (60F254), using UV light (254 nm) and phosphomolybdic acid as developing agent. Flash column chromatography using E. Merck silica gel 60H was performed by gradient elution of mixture of *n*-hexane and increasing volumes of dichloromethane or ethyl acetate. Reactions were run under an argon atmosphere with freshly anhydrous distilled solvents, unless otherwise noted. Yields refer to chromatographically and spectroscopically homogeneous materials, unless otherwise stated.

Synthesis of Dendrimer 1 by Hydrogenation of Dendrimer 3. Dendrimer 3 29.9 mg (0.025 mmol) was dissolved in distilled ethyl acetate (30.0 mL) and 19.5 mg of Pd/C 10% were added. The fluorescent mixture was degassed by 5 cycles of hydrogen-vacuum and then stirred under atmospheric pressure of hydrogen for 2 days. The colorless mixture was filtered through a Celite pad, washed with chloroform and the solvents were concentrated under reduce pressure. Crude product (35.5 mg) was purified by column chromatography yielding 24.5 mg (0.020 mmol, 81%) of dendrimer 13 as colorless oil. ¹H NMR, δ (300 MHz, CDCl₃, TMS): 7.23 (*sa*, SH), 7.21 (s, 4H), 7.13 (s, 11H), 7.07 (*d*, J = 8.85 Hz, 20H), 7.04–6.95 (*m*, 14H), 6.85 (s, 3H), 2.88 (s, 10H), 2.86 (s, 14H). ¹³C NMR, δ (75 MHz, CDCl₃, TMS): 148.01, 145.70, 141.87, 139.55, 139.40, 136.67, 129.24, 129.14, 128.47, 128.34, 126.31, 124.67, 123.78, 122.35, 38.08, 37.74, 37.58, 37.47. MALDI-TOF (*m/e*): calcd for C₉₀H₈₁N₃, 1204.6 (M⁺); obsd, 1204.5 (M⁺).

Synthesis of Dendrimer 2. To a mixture of 13 (64.8 mg, 0.07 mmol) in dry toluene were added triethylamine 1:1 (14 mL) Pd(PPh₃)₄ (11.4 mg, 0.01 mmol), CuI (2.4 mg, 0.01 mmol), and triphenylphosphine (2.5 mg, 0.01 mmol), and the mixture was stirred for 15 min under argon atmosphere. Commercial phenylacetylene (0.05 mL, 0.43 mmol) was added and the reaction was stirred overnight at 80 °C at this temperature. The solvent was evaporated and the crude product was purified by column chromatography yielding 51.7 mg (0.06 mmol, 87%) of dendrimer 2 as yellow solid. Mp: 122–125 °C. ¹H NMR, δ (300 MHz, CDCl₃, TMS): 7.56–7.52 (*m*, 7H), 7.50 (*d*, J = 4.6 Hz, 9H), 7.47–7.40 (*m*, 8H), 7.38–7.32 (*m*, 9H), 7.16–7.07 (*m*, 9H), 7.01 (*d*, J = 16.3 Hz, 3H). ¹³C NMR, δ (75 MHz, CDCl₃, TMS): 146.81, 137.48, 132.06, 131.95, 131.60, 128.90, 128.37,

128.25, 127.63, 126.75, 126.26, 124.31, 123.34, 122.00, 90.28, 89.64. MALDI-TOF (*m/e*): calcd for C₉₀H₆₃N₃, 1186.5 (MH⁺); obsd, 1186.4 (MH⁺).

Synthesis of Dendrimer 3. To a solution of 15 (231.0 mg, 0.49 mmol) in dry toluene:triethylamine 1:1 (16 mL) were added Pd(PPh₃)₄ (18.3 mg, 0.02 mmol) and CuI (4.3 mg, 0.02 mmol), and the mixture was stirred for 15 min under argon atmosphere at room temperature. 1,3,5-Triethynylbenzene (7) (18.4 mg, 0.12 mmol) was added and the reaction was refluxed during 48 hs. The solvent was evaporated and the crude product was purified by column chromatography yielding 80.3 mg (0.07 mmol, 55%) of dendrimer (3) as orange solid. Mp: 135–138 °C.

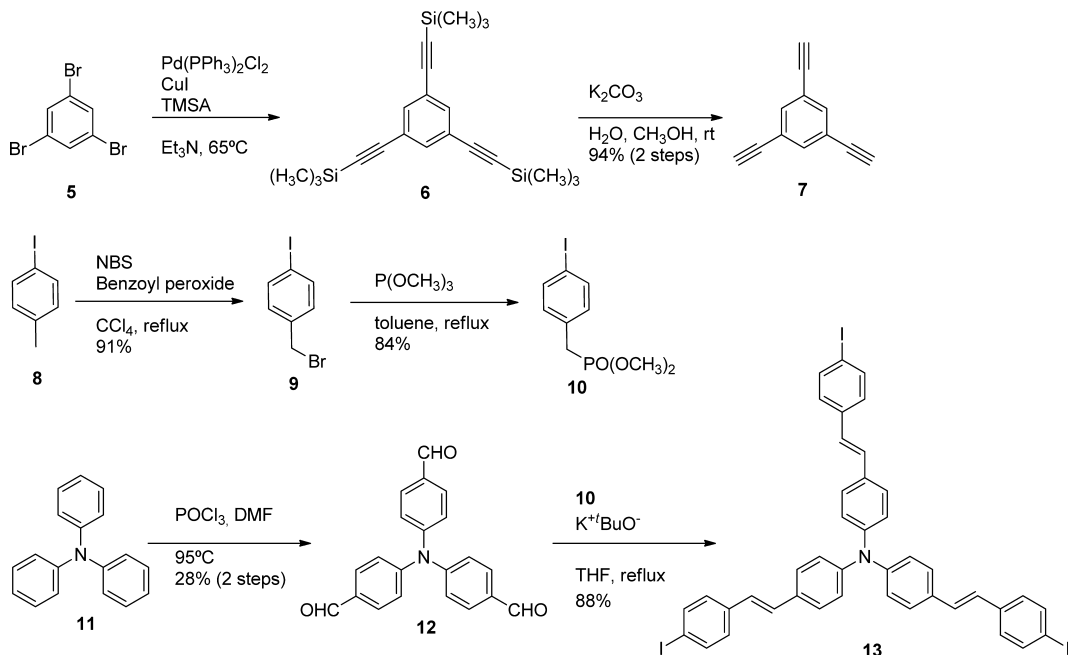
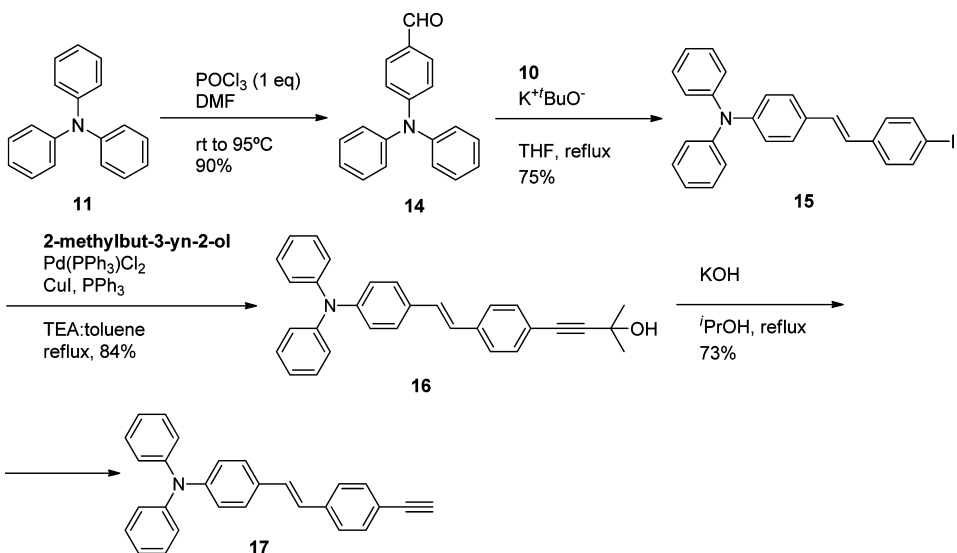
¹H NMR, δ (300 MHz, CDCl₃, TMS): 7.64 (s, 3H), 7.48 (*dd*, J = 12.1 Hz, J = 8.6 Hz, 12H), 7.38 (*d*, J = 8.6 Hz, 7H), 7.34–7.23 (*m*, 8H), 7.14–7.09 (*m*, 14H), 7.07–6.99 (*m*, 18H), 6.94 (s, 1H). ¹³C NMR, δ (75 MHz, CDCl₃, TMS): 147.69, 147.48, 137.99, 133.91, 132.05, 131.06, 129.34, 127.54, 126.26, 126.14, 124.65, 124.14, 123.36, 123.20, 121.34, 90.86, 88.73. MALDI-TOF (*m/e*): calcd for C₉₀H₆₃N₃, 1186.5 (MH⁺); obsd, 1186.4 (MH⁺).

Synthesis of Dendrimer 4. To a mixture of 13 (34.9 mg, 0.038 mmol) in dry toluene were added triethylamine 1:1 (14 mL) Pd(PPh₃)₄ (7.0 mg, 0.006 mmol), CuI (2.0 mg, 0.011 mmol), and triphenylphosphine (1.0 mg, 0.004 mmol), and the mixture was stirred for 15 min under argon atmosphere at room temperature. Dendron 17 (63.0 mg, 0.167 mmol) was added and the reaction stirred and refluxed overnight. After solvent evaporation, the crude product was purified by column chromatography and crystallized by dichloromethane: hexane yielding 51.7 mg (0.024 mmol, 63%) of dendrimer 4. The solid was recrystallized from acetone: hexanes yielding 39.8 mg of 4 as an orange solid. Mp: 200–203 °C. ¹H NMR, δ (300 MHz, CDCl₃, TMS): 7.58–7.33 (*m*, 35H), 7.32–7.20 (*m*, 14H), 7.19–6.90 (*m*, 41H). ¹³C NMR, δ (75 MHz, CDCl₃, TMS): 147.61, 147.48, 146.74, 137.58, 138.39, 132.05, 131.95, 131.12, 129.34, 129.08, 128.87, 127.67, 127.52, 126.77, 126.33, 126.26, 124.63, 124.31, 123.38, 123.18, 122.09, 121.89, 90.73, 90.59. MALDI-TOF (*m/e*): calcd for C₁₂₆H₉₀N₄, 1658.7 (M⁺); obsd, 1658.4 (M⁺).

Optical Characterization. Absorption and fluorescence spectra were recorded on a Shimadzu UV-2401PC spectrometer and on a Spex FluoroMax fluorometer, respectively. Spectra were recorded using quartz cells (path length: 1 cm) using 1,2-dichloroethane (DCE) as a solvent at room temperature.

Electrochemical Study and Polymer Films Electrodeposition. The redox properties of dendrimers were studied in 0.5–1.0 mM range concentration in DCE solution containing 0.1 M tetra-*n*-butylammonium hexafluorophosphate (TBAHFP) as support electrolyte using a potentiostat Autolab Electrochemical Instruments. The working electrode consisted of a 2.16 \times 10⁻³ cm² inlaid platinum disk that was polished on a felt pad with 0.3 μ m alumina and sequentially sonicated in water and absolute ethanol for 3 min each; and finally dried with a hot air gun. The voltammetric experiments were carry out using a silver wire as pseudoreference electrode and a platinum coil was used as the counter electrode. Cyclic potential scans were made in the electrochemical windows of the system solvent–electrolyte in order to discard possible active electrochemically interferes. All potential values in this study are expressed relative to a ferrocene/ferrocenium redox couple (Fc/Fc⁺ = 0.40 V vs SCE) that was added to the solution as an internal standard.³⁵ The molecules studied were electropolymerized on Pt and ITO (indium tin oxide, Delta Technologies, nominal resistance 10 Ω /square) electrodes by cyclic voltammetry technique under the experimental conditions described above.

Spectroelectrochemical. The experiments were carried out in a homemade cell built from a commercial UV-visible cuvette. The ITO-coated glass with a polymer film was used as working electrode, the Pt counter electrode was isolated from the monomer solution by a glass frit, and a silver wire was used as pseudoreference electrode. The cell was placed in the optical path of the sample light beam. The background correction was obtained by taking an UV-visible spectrum of a blank cell (an electrochemical cell with an ITO working

Scheme 1. Synthesis of Cores 7 and 13**Scheme 2. Synthesis of Dendrons 15 and 17**

electrode without the polymer film) working under the similar conditions and parameters for polymer experiments cited above.

Film Analysis. Topography of electrodeposited polymer films was performed by scanning electron microscopy (SEM). The samples were analyzed on a Carl Zeiss EVO MA 10 with electron beam energy of 18 KV.

RESULTS AND DISCUSSION

Synthesis and Characterization of Dendrons and Dendrimers. All dendrimers (Figure 1) were obtained by Sonogashira coupling between cores 1,3,5-triethynylbenzene (TEB) (7) or tris{4-[*E*-2-(4-iodophenyl)vinyl]phenyl}amine (13) and the corresponding dendrons. The core 7 was prepared according to a synthetic protocol³⁶ starting from commercial 1,3,5-tribromobenzene (5) as described in Scheme 1. The product 7 was obtained in two steps with 94% as overall yield. Core 13 was synthesized from tris(4-formylphenyl)amine

12 prepared from the product of the Vilsmeier–Haack formylation of commercial triphenylamine 11.³⁷ Then, Wadsworth–Horner–Emmons reaction³⁸ of this tris-formyl derivative 12 with phosphonate 10³⁹ allowed us to obtain compound 13 in very good yield (88%, Scheme 1).

Synthesis of dendrons 15 and 17 were accomplished as described in Scheme 2. Dendron 15 was obtained via Wadsworth–Horner–Emmons reaction with phosphonate 10³⁹ of the formyl derivative 14⁴⁰ in 75% yield. Dendron 17 was synthesized starting with the Sonogashira reaction of 15 with the terminal protected alkyne 2-methylbut-3-yn-2-ol yielding 16 in 84% yield. Deprotection of 16 with potassium hydroxide³⁸ afforded 17 in 73% yields.

Taking into account that phosphonate carbanions produce predominately *E* stereochemistry of double bonds, a stabilized phosphorus ylide was chosen instead of Wittig protocol because

Scheme 3. Synthesis of Dendrimers 1, 2, 3, and 4

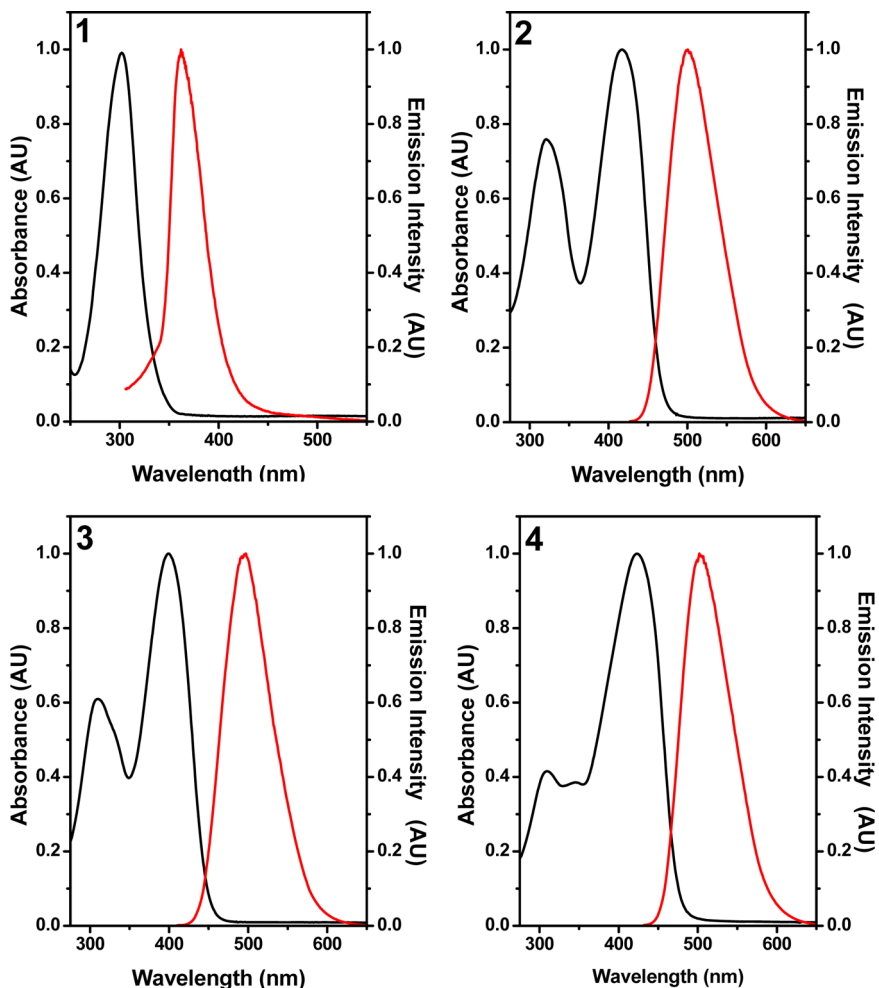
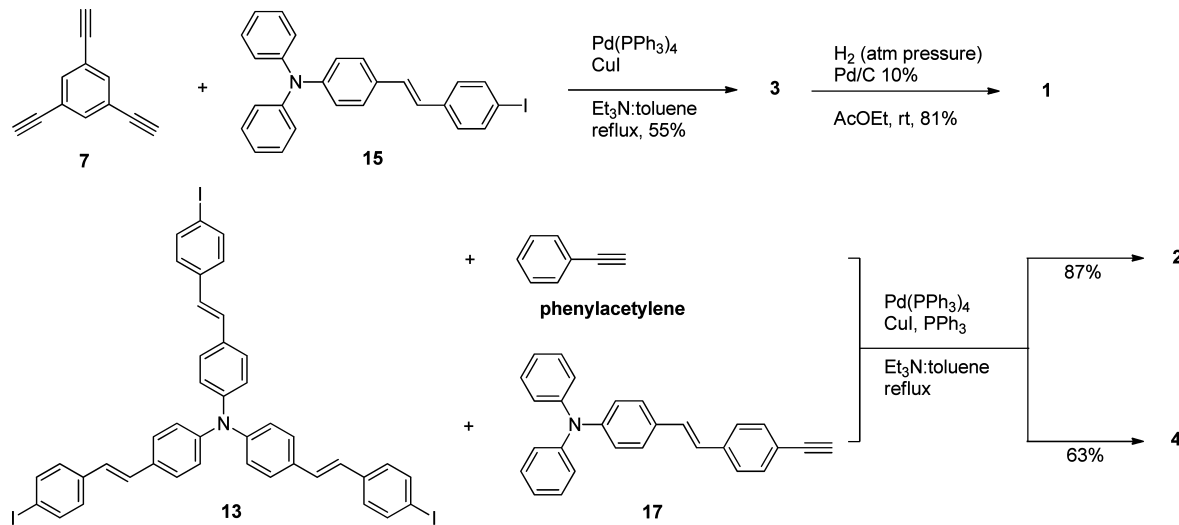


Figure 2. UV visible absorption and emission spectroscopy DCE in solution Normalized absorption (black line) and emission (red line) spectra of studied dyes in DCE solution. The emission spectra were measured by excitation at the maximum of the lower energy bands.

better yields and regioselectivity of the alkene derivatives were obtained.

Dendrimer 3 was prepared through a carbon–carbon coupling reaction of the core 7 and dendron 15 using $\text{Pd}(\text{PPh}_3)_4$ and CuI in toluene: triethylamine solvents mixture

(Scheme 3). The product was isolated after column chromatography purification yielding 3 as orange solid in 55% yield. Dendrimers 2 and 4 were obtained under similar Sonogashira coupling conditions between the nucleus 13 and commercial phenylacetylene yielding 2 as a yellow solid in 87%

yield (after column chromatography purification) and carbon–carbon coupling reaction of **13** with dendron **17** afforded dendrimer **4** as an orange solid in 63% yield after crystallization. Catalytic hydrogenation of **3** with hydrogen under atmospheric pressure using Pd/C as catalyst in ethyl acetate as solvent afforded dendrimer **1** in 81% yield as a colorless oil (Scheme 3). The structures of the cores and dendrons were confirmed by ¹H NMR, ¹³C NMR spectroscopy and low resolution mass spectrometry experiments and compared with the corresponding bibliographic reference when necessary. Structures of dendrimers were characterized by ¹H NMR, ¹³C NMR, and MALDI–TOF mass spectrometry experiments. In the conjugated macromolecules **2**, **3**, and **4** the observation of two sp carbons corresponding to alkyne signals and the total number of different carbon atoms signals in the ¹³C NMR spectrum allowed us to confirmed the starburst structure of dendrimers. Dendrimer **1** showed no alkyne signals in ¹³C NMR spectrum and four new methylene peaks were observed. In the ¹H NMR spectrum broad signals at 2.86 and 2.88 ppm corresponding to a total of 24 protons demonstrated the completed hydrogenation of all the alkenes and alkynes present in the starting material **3**. MALDI–TOF data confirmed the expected molecular mass calculated for each dendrimer. Experimental details for nuclei and dendrons synthesis and NMR data are described in the Supporting Information.

Dendrimers Optical Properties. UV–visible absorption and emission spectroscopy measurements were performed both in solution and in solid films for the electrodeposited polymers. The absorption and fluorescence spectra of this set of molecules in DCE solution is shown in Figure 2, and the main optical characteristics are summarized in Table 1. The

Table 1. Absorption and Emission Characteristics of the Studied Dendrimers

compound	λ_{\max} absorption (nm)		λ_{\max} emission (nm) ^b	
	toluene	DCE	toluene	DCE
1^a	302	302	357	362
2	319/413	321/416	463	500
3	308/399	310/399	450	493
4	310/346/423	310/344/423	469	503

^aMeasured in cyclohexane. ^bThe emission spectra were measured by excitation at the maximum of the lower energy bands.

dendrimers studied possess different structural characteristics. Compound **2** hold sonly a TPA moiety in the core, while **1** and **3** have their TPA groups as outer substituent in the dendrimeric structure. The main difference between dendrimers **1** and **3** is the lack of conjugated branches in the first one. Finally, dendrimer **4** shows fully conjugated TPA groups both in the core and in the outer layer.

The analysis of the absorption spectra permits to observe that **1** showed a single light absorption peak, while **2**, **3**, and **4** showed two optical transitions, one with maximum around of $\lambda = 300$ nm and other approximately at 400 nm. Therefore, the high energy bands in the dendrimers can be assigned to light absorption by the triphenylamine moieties, and the lower energy bands to $\pi-\pi^*$ transitions.^{41,42} The observed differences between the wavelength maximum in Table 1 are related to the effective conjugation lengths and group interaction effects. An analysis in DCE, revealed that the band ascribed to TPA absorption in **3** is 8 nm red-shifted respects to this band in **1** spectrum due the presence of one conjugated vinylene with the

TPA moieties. In dendrimer **2**, which holds one TPA unit as core, the high energy band moves to lower energy (321 nm, 19 nm red-shifted with respect **1** molecule), due to the presence of three vinylene-modified phenyls groups in the TPA. Finally, the spectrum of **4** showed a band with maximum at $\lambda = 310$ nm which can be ascribed to the outer TPA moieties with one conjugated vinylene group, similar to those observed in **3**. Also, an additional peak at λ_{\max} at 344 nm was presents in **4**. This transition can be assigned to the vinylene-modified the TPA core. The molecular structure of **4** can be seen as combination of **2** and **3**, since its core is similar to **2** and the periphery or shell resembles to **3**. However, Figure 2 shows that light absorption spectrum of **4** is not a lineal combination of **2** and **3** spectra (See Table 1), which indicates that the conjugated linker allows interaction between the core and the periphery of the dendrimer. On the other hand, the low energy bands ($\lambda_{\max} \sim 400$ nm) that are present in all dendrimers except **1**, showed similar behaviors (see Table 1): a red shift is detected in these $\pi-\pi^*$ transitions with the increment of conjugation length. This tendency was observed in low and high polarity solvents (toluene and DCE).

In addition, Figure 2 showed the photoluminescence spectra of monomers in diluted DCE solutions measured by excitation at the absorption maximum wavelength of the $\pi-\pi^*$ transitions, except for **1**, which was excited at maximum of the light absorption by the TPA moieties. For **2**, **3** and **4**, maximum bands for emission were detected at 493, 500, and 503 nm, respectively. Thus, the fluorescence spectra also showed the effect of the difference in effective conjugation length observed in absorption spectra. Furthermore, marked red shifts was observed in the emission maxima when the fluorescence spectra were measured in DCE with respect to the same obtained in lower polarity medium (toluene, see Table 1), which is in according with the properties of $\pi-\pi^*$ transitions.

Dendrimers Electrochemical Characterization and Electrodeposition of Polymeric Films. Redox properties and radical ions stability of the dendrimers were determined by cyclic voltammetry in DCE solution containing TBAHPP 0.1 M as supporting electrolyte at room temperature, using a Pt disk as a working electrode. Dendrimer **3** holds three TPA units as electroactive group in their periphery; therefore, it is expected that their oxidation behavior is ruled by these groups. Figure 3a showed two consecutive cyclic voltammograms of **3**. In the first anodic scan, multiples oxidation peaks at 0.31, 0.43, and 0.64 V are observed. When the potential scan is inverted three reduction waves can be detected with peaks at 0.36, 0.11, and -1.04 V. The second scan shows a similar profile, but with a remarkable growing in the current. The electro-oxidation of TPA was extensively studied,^{43,44} and it is known that the radical cation formed by oxidation can be involved in a dimerization reaction which produced tetraphenylbenzidine (TPB) derivatives.^{27–47}

Also, the generated TPB is an electroactive center that undergoes two successive reversible oxidation processes, which are responsible of the additional waves observed in cyclic voltammetry of **3**.^{27–45} This mechanism allows the growing of a electroactive polymeric structure when **3** is successively cycled between -1.6 and 0.9 V. Typical multiple CV scans of this compound on a Pt electrode are shown in Figure 3b. In addition to the TPA dimerization mechanism, it is known that TPA exhibits reactivity in the dicationic charged state, with simultaneous parallel follow-up coupling reactions, which was careful described in a recent paper by Yurchenko et al.⁴⁸ These

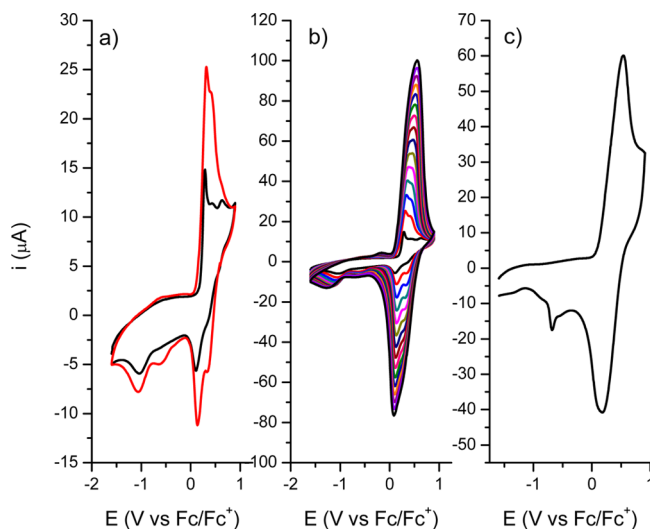


Figure 3. Cyclic voltammogram of the compound 3: (a) first (black) and second (red) cycles; (b) repetitive cyclicvoltamograms. (c) Cyclic voltammogram of the electro-deposited film derived from 3 on a Pt electrode in DCE with 0.1 M of TBAHPP, $v = 0.1 \text{ V s}^{-1}$.

follow-up coupled reactions could contribute to the voltametric waves associated with the main process. To confirm the existence of an electroactive dendrimeric polymer, the working electrode was transferred to a supporting electrolyte solution free of monomer. The redox response of this modified electrode is shown in Figure 3c where it can be observed one oxidation peaks at 0.56 V and one catodic waves at 0.18 V. These observations confirms that the oxidation process of TPA outer layer results in the formation of TPB through a dimerization reaction, which leads to the formation of a stable and electroactive film on electrode surface.

Similarly to 3, dendrimer 4 has three TPA groups in the outer layer of the dendrimer, but it holds an additional electroactive triphenylamine as central core. Consequently, 4 showed a similar electrochemical behavior, producing three oxidation waves in the first cycle (Figure 4a), two peaks are

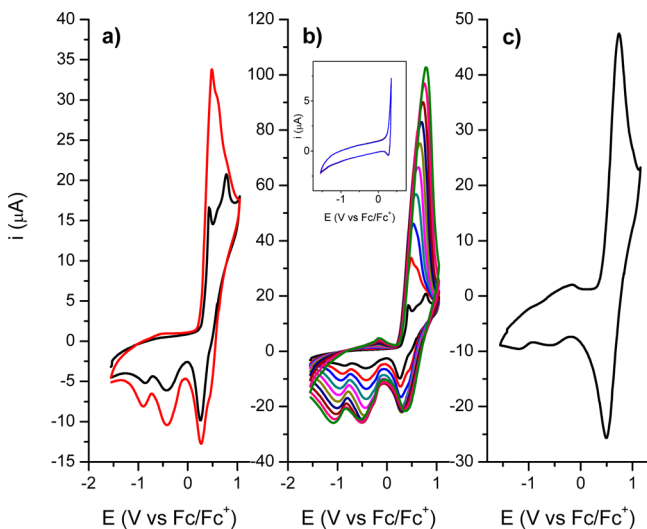


Figure 4. Cyclic voltammogram of the compound: (a) first (black) and second (red) cycles; (b) repetitive cyclicvoltamograms. (c) Cyclic voltammogram of the electro-deposited film derived from 4 on a Pt electrode in DCE with 0.1 M of TBAHPP, $v = 0.1 \text{ V s}^{-1}$.

defined at 0.42 and 0.77 V and one is manifested as shoulders at 0.65 V. In the reverse scan three peaks are observed as complementary reduction processes at +0.25, -0.43, and -0.86 V, showing an irreversible behavior typical of chemical reactions coupled to the heterogeneous charge transfer. Therefore, these results suggest that oxidation of the central core and the periphery groups occurs at a similar applied potential in compound 4, and also undergoes an analogous electropolymerization process. This assumption was confirmed by the increasing current observed in the second CV scan (Figure 4a), and by the growing of an electroactive polymeric structure when 4 was successively cycled between -1.6 and +1.0 V (Figure 4b).

Additionally, the electrochemical study of dendrimer 2, which also holds TPA core but lacks of peripheral electroactive groups, showed (Figure 5) a quasireversible oxidation wave at

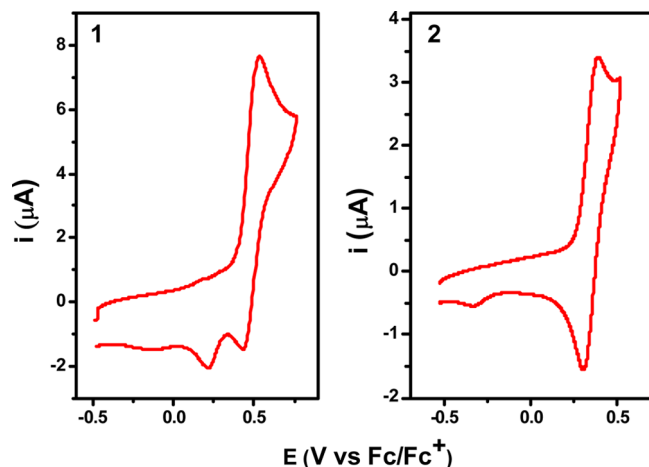


Figure 5. Cyclic voltammogram of the molecules 1 and 2 in DCE with 0.1 M of TBAHPP, on Pt electrode at a scan rate of 100 mV/s.

0.38 V. This behavior is expected because dendrimer 2 has an amine group with blocked phenyl rings in the reactive *para*-position which allows to form stable oxidized states.^{29–48} Thus, in 4 dendrimer, the core oxidation should occur at a similar applied potential. This is evidenced when the potential is cycled until the first oxidation wave obtaining a reversible response without film formation (see inset in Figure 4b). This conclusion is also supported by the spectroelectrochemical studies carried out on the electropolymerized films (see below).

As it was done with compound 3, with the aim of study the electrochemical behavior of the electrogenerated polymer of 4, the working electrode was removed and washed with DCE in order to eliminate residual monomer content. Subsequently, it was transferred to a three-electrode cell with supporting electrolyte solution free of monomer to study the film redox behavior. Figure 4c shows the film response, which confirms that the oxidation processes of macromolecule 4 forms an irreversibly adsorbed electroactive product on the electrode surface. The film has a reversible oxidation wave with a potential peak at 0.77 V, and shows a great stability when the film is submitted to numerous oxidation-reduction cycles.

In the electrooxidation of the hydrogenated dendrimer 1, which has a nonconjugated structure with TPA peripheral groups, no stable film formation was obtained under the present experimental conditions, in spite that the TPA substituent oxidation drives to the radical cation coupling and

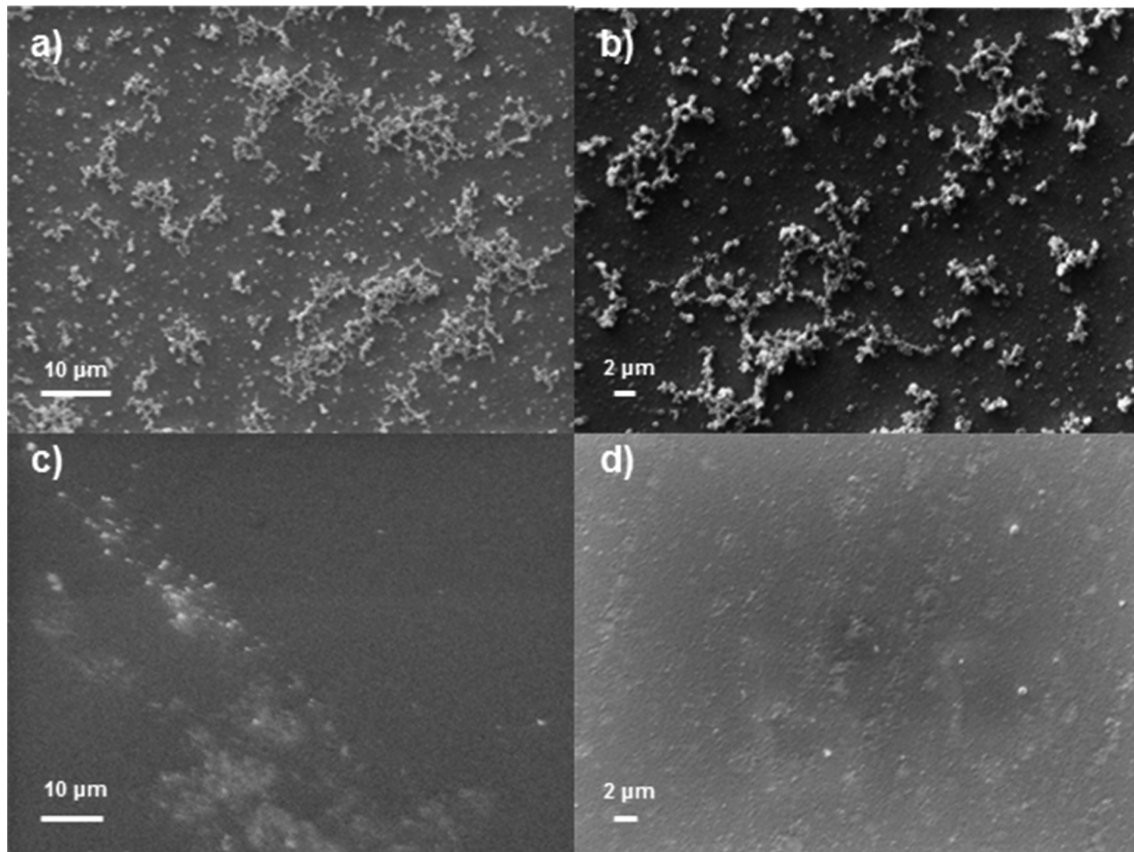


Figure 6. SEM images of the molecules obtained at different magnifications of the films obtained from **4** (a, b) and **3** (c, d).

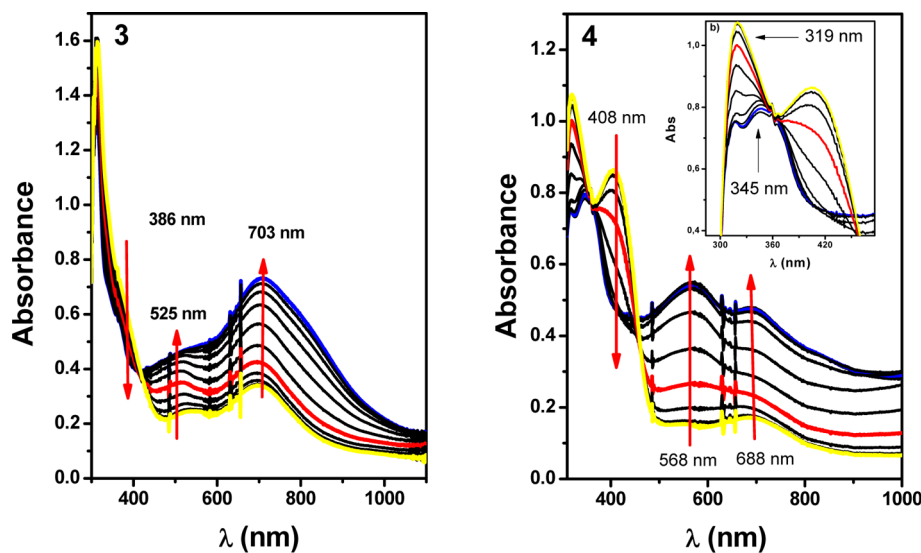


Figure 7. Absorption spectra of electrodeposited films on an ITO electrode at different applied potentials of the compounds **3** and **4**.

TPB formation. This fact is corroborated by the typical two reduction waves observed in the reverse scan^{43,45} (Figure 5b).

It is possible to suppose that the dimers and/or oligomers formed in the electrode–solution interface are soluble, and the metal surface–organic molecule interaction in this case is not strong enough to allow film formation. The higher solubility of dimers and/or oligomers of **1** could be related to the higher rotational and conformational freedom degrees of this dendrimer in comparison with related compounds **3** and **4**. Tridimensional idealized structures obtained by molecular

mechanic calculation (MM^+) of the dendrimer **1** and **3** (see Figure S20 in Supporting Information) show that in the case of **1** a globular shape is permitted because the rotational freedom of the single bonds. Contrarily, in **3**, a rigid star shape is observed due to the multiple conjugated bonds present in the dendrimer arms. It is possible that the globular fashion in **1** contributes to increase the solubility of the electrooxidation products, affecting the film formation on the electrode surface. These results indicate that, when designing a dendron, the use

of conjugated and hence more rigid structures is an important factor in order to obtain electropolymeric films.

Surface Analysis of Electrogenerated Films. It is well-known that the morphology of organic polymeric films plays a key role when they are used as components in optoelectronics devices. The presence of cracks, pinholes or inhomogeneities in the surface can produce electrical shortcuts or current paths with different resistances, which affects the performance and stability of the devices.^{28,27} The surface morphology of 3 and 4 polymeric films were analyzed by scanning electron microscopy (SEM) and the obtained images are shown in Figure 6. In both cases the polymeric structure full covered the ITO electrode surface, without unfilled spaces. However, different morphologies can be easily perceived. In the film derived from dendrimeric compound 3, the images in Figure 6, parts a and b, showed the presence of an inhomogeneous and granulate surface. The micrograph allowed to see irregularly shaped grains. On the other hand, SEM images of polymer of 4 (Figure 6, parts c and d) shows a smooth surface, without grains, cracks, or pinholes. It can be seen that the film fully covers the ITO electrode, without leaving islands, and the surface morphology is completely soft and free of agglomerations. These facts were repetitive for all the formed films, although the growing conditions (monomer concentration, solvent and electrolyte) for both films were the same. Thus, the differences observed in films morphology are related to the molecular structure of the dendrimers. As it was previously mentioned, the main difference is the presence of the TPA electroactive central core in 4. As it is demonstrated by electrochemical and spectroelectrochemical studies (see below), this core is oxidized during the electrodeposition procedure. The positive charge located in the central core could produce columbic repulsion between different polymeric branches, with effect over both, the nucleation and growing processes of the film, affecting their surface morphology.

Spectroelectrochemical Characterization of Electro-generated Films. Spectroelectrochemical studies of the electrodeposited films on ITO electrode were performed in order to obtain information about the polymer molecular structure and polymerization mechanism. Figure 7 shows the absorption spectra at different applied potentials electro-polymerized films obtained from 3 and 4.

The absorption spectra of the films were obtained as a function of applied potentials between 0 and \sim 1.3 V. The films in their neutral state (0 V) are semitransparent (they show a pale yellow color to the naked eye), with light absorption at λ bellow \sim 450 nm assigned to π - π^* transition. As the potential is increased to positive values, the intensity of these bands decrease, while new bands appear, in the wavelength range from 400 to 1000 nm, which produced a visible change in the color of the films from yellow to red and finally to blue (Figure 7). The absorption spectra of the electrodeposited film of dendrimer 3 revealed a decrease in intensity of the shoulder at 386 nm (that extends to the visible region) when the applied potential became more anodic, while an increase of the two absorption bands at $\lambda_{\text{max}} = 525$ and 703 nm was observed. The intensity of the second absorption peak rises and reaches a maximum at 1.2 V. This absorption is ascribed to the fully oxidized state of the electro-deposited film of 3. All these results are in fully agreement with the presence of TPB in the film's molecular structures.^{29,45,48,47} Neutral TPB shows an absorption band with $\lambda_{\text{max}} = 352$ nm; meanwhile, the TPB radical

holds absorption with $\lambda_{\text{max}} = 484$ cation and the dication at 450 and 722 nm.⁴⁸

The spectroelectrochemical response of polymer derived from compound 4 showed different features with respect to those observed for dendrimer 3. In the neutral form a sharp band with $\lambda_{\text{max}} = 319$ nm is observed, which decreased upon film oxidation. Concomitantly, a new band with $\lambda_{\text{max}} = 345$ nm is formed (inset in Figure 7). These results are in agreement with an electrochemical process associated with TPA central core of the dendrimer. The 319 nm band can be assigned to the TPA in neutral forms; meanwhile the band at 345 nm is typical of TPA cation radical. Furthermore, the absorption bands detected at $\lambda_{\text{max}} = 568$ and 688 nm also are related to the formation of TPA cation radical. In parallel to the dendrimer central core electrochemical process, the characteristic neutral TPB absorption band, centered at $\lambda_{\text{max}} = 405$ nm, decreased as the applied potential becomes more anodic. The TPB cation radical and dication absorption are superimposed with the long wavelength TPA radical cation absorption bands. These facts indicated that this conductive dendritic polymer can be reversibly charged, both in the core and in the peripheral units. This polymer is fully conjugated with a starburst structure that can prevent staking or aggregation between the redox centers. These characteristics are of great importance in order to obtain adequate charge transporting and optoelectronic properties, which in turns are inherent to the development of materials that could have applications in organic electronic and optoelectronic devices.

CONCLUSION

A series of electroactive dendrimers was obtained by a versatile convergent synthetic strategy which involved Sonogashira cross coupling reaction to assemble the dendrons with the core. Dendrons were easily prepared following standard synthetic procedures. The studied compounds contain a branched structure with multiple TPA groups, which allows independent dimerization and electropolymerization reaction that modifies the electrode surfaces with conductive electropolymers. The dendrimer structures were systematically modified, and relationships between optical, electrochemical and film surface morphological characteristics with the molecular structural parameters were established. This work provides a model to design starburst dendrimers capable to form electrochemically active polymers. These results showed that the rigidity reach by the extended conjugation in dendrimer branches is a key factor to obtain polymers films by electrodeposition technique. Also, the presence of charged center in the dendrimer core can affect the electropolymer surface quality film formation. A polymeric material with smooth surface, good electrical conductivity and stability was obtained. These material characteristics are of great relevance for their potential application in the development of organic optoelectronic devices.

ASSOCIATED CONTENT

Supporting Information

Synthetic procedures and characterization data, ^1H and ^{13}C NMR spectra, and MM⁺ calculation of the synthesized compounds. This material is available free of charge via the Internet at <http://pubs.acs.org>

AUTHOR INFORMATION

Corresponding Author

*E-mail: (R.A.S.) spanevello@iquir-conicet.gov.ar; (F.F.) ffungo@exa.unrc.edu.ar.

Notes

The authors declare no competing financial interest.

ACKNOWLEDGMENTS

We thank Consejo Nacional de Investigaciones Científicas y Técnicas (CONICET-Argentina), Agencia Nacional de Promoción Científica y Tecnológica (ANPCYT Argentina), and Universidad Nacional de Rosario y Universidad Nacional de Río Cuarto. M.I.M., R.A.S., L.F., L.O., and F.F. are scientific members of CONICET.

REFERENCES

- (1) D'Andrade, B. W.; Forrest, S. R. *Adv. Mater.* **2004**, *16*, 1585–1595.
- (2) Walzer, K.; Maennig, B.; Pfeiffer, M.; Leo, K. *Chem. Rev.* **2007**, *107*, 923–1386.
- (3) Hwang, S.-H.; Moorefield, C. N.; Newkome, G. R. *Chem. Soc. Rev.* **2008**, *37*, 2543–2557.
- (4) Kulkarni, A. P.; Tonzola, C. J.; Babel, A.; Jenekhe, S. A. *Chem. Mater.* **2004**, *16*, 4556–4573.
- (5) Sudyoedsuk, T.; Promarak, V. *Chem. Commun.* **2012**, *48*, 3382–3384.
- (6) Albrecht, K.; Pernites, R.; Felipe, M. J.; Advincula, R. C.; Yamamoto, K. *Macromolecules* **2012**, *45*, 1288–1295.
- (7) Svenson, S. *Eur. J. Pharm. Biopharm.* **2009**, *71*, 445–462.
- (8) Langereis, S.; Dirksen, A.; Hackeng, T. M.; Van Genderen, M. H. P.; Meijer, E. W. *New J. Chem.* **2007**, *31*, 1152–1160.
- (9) Balzani, V.; Bergamini, G.; Ceroni, P.; Marchi, E. *New J. Chem.* **2011**, *35*, 1944–1954.
- (10) Reek, J. N. H.; Arévalo, S.; van Heerbeek, R.; Kamer, P. C. J.; van Leeuwen, P. W. N. M. *Adv. Catal.* **2006**, *49*, 71–151.
- (11) Jin-Liang Wang, Yi Zhou; Yongfang, Li; Jian, Pei. *J. Org. Chem.* **2009**, *74*, 7449–7456.
- (12) Qin, T.; Wiedemair, W.; Nau, S.; Trattning, R.; Sax, S.; Winkler, S.; Vollmer, A.; Koch, N.; Baumgarten, M.; List, Emil J. W.; Mullen, K. *J. Am. Chem. Soc.* **2011**, *133*, 1301–1303.
- (13) Adhikari, R. M.; Mondal, R.; Shah, B. K.; Neckers, D. C. *J. Org. Chem.* **2007**, *72*, 4727–4732.
- (14) Kwon, T.-W.; Alam, M. M.; Jenekhe, S. A. *Chem. Mater.* **2004**, *16*, 4657–4666.
- (15) Burn, P. L.; Lo, S.-C.; Samuel, I. D. *Adv. Mater.* **2007**, *19*, 1675–1688.
- (16) Lo, S.-C.; Burn, P. L. *Chem. Rev.* **2007**, *107*, 1097–1116.
- (17) Nakashima, T.; Satoh, N.; Albrecht, K.; Yamamoto, K. *Chem. Mater.* **2008**, *20*, 2538–2543.
- (18) Lu, J.; Xia, P. F.; Lo, P. K.; Tao, Y.; Wong, M. S. *Chem. Mater.* **2006**, *18*, 6194–6203.
- (19) Rajakumar, P.; Thirunarayanan, A.; Raja, S.; Ganesan, S.; Maruthamuthu, P. *Tetrahedron Lett.* **2012**, *53*, 1139–1143.
- (20) Thelakkat, M. *Macromol. Mater. Eng.* **2002**, *287*, 442–461.
- (21) Shirota, Y. *J. Mater. Chem.* **2000**, *10*, 1–25.
- (22) Kuwahara, Y.; Ogawa, H.; Inada, H.; Norma, N.; Shirota, Y. *Adv. Mater.* **1994**, *6*, 677–679.
- (23) Adachi, C.; Nagui, K.; Tamoto, N. *Appl. Phys. Lett.* **1995**, *66*, 2679–2681.
- (24) Fenter, P.; Schreiber, F.; Bulovic, V.; Forrest, S. R. *Chem. Phys. Lett.* **1997**, *277*, 521–526.
- (25) Adachi, C.; Tsutsui, T.; Saito, S. *Appl. Phys. Lett.* **1990**, *56*, 799–782.
- (26) Tokito, S.; Taga, Y. *Appl. Phys. Lett.* **1995**, *66*, 673–676.
- (27) Heredia, D.; Fernandez, L.; Otero, L.; Ichikawa, M.; Lin, C.-Y.; Liao, Y.-L.; Wang, S.-A.; Wong, K-T.; Fungo, F. *J. Phys. Chem. C* **2011**, *115*, 21907–21914.
- (28) Li, M.; Tang, S.; Shen, F.; Liu, M.; Xie, W.; Xia, H.; Liu, L.; Tian, L.; Xie, Z.; Lu, P.; Hanif, M.; Lu, D.; Cheng, G.; Ma, Y. *J. Phys. Chem. B* **2006**, *110*, 17784–17789.
- (29) Gervaldo, M.; Funes, M.; Durantini, J.; Fernandez, L.; Fungo, F.; Otero, L. *Electrochim. Acta* **2010**, *55*, 1948–1957.
- (30) Liddell, P. A.; Gervaldo, M.; Bridgewater, J. W.; Keirstead, A. E.; Lin, S.; Moore, T. A.; Moore, A. L.; Gust, D. *Chem. Mater.* **2008**, *20*, 135–142.
- (31) Tang, S.; Liu, M.; Lu, P.; Xia, H.; Li, M.; Xie, Z.; Shen, F.; Gu, C.; Wang, H.; Yang, B.; Ma, Y. *Adv. Funct. Mater.* **2007**, *17*, 2869–2877.
- (32) Li, M.; Tang, S.; Shen, F.; Liu, M.; Li, F.; Lu, P.; Lu, D.; Hanif, M.; Ma, Y. *J. Electrochem. Soc.* **2008**, *155*, H287–H291.
- (33) Gu, C.; Tang, S.; Yang, B.; Liu, S.; Lu, Y.; Wang, H.; Yang, S.; Hanif, M.; Lu, D.; Shen, F.; Ma, Y. *Electrochim. Acta* **2009**, *54*, 7006–7011.
- (34) Nonami, H.; Fukui, S.; Erra-Balsells, R. *J. Mass Spectrom.* **1997**, *32*, 287–296.
- (35) Cardona, C. M.; Li, W.; Kaifer, A. E.; Stockdale, D.; Bazan, G. C. *Adv. Mater.* **2011**, *23*, 2367–2371.
- (36) Kobayashi, N.; Kijima, M. *J. Mater. Chem.* **2008**, *18*, 1037–1045.
- (37) Malegol, T.; Gmouh, S.; Meziane, M. A. A.; Blanchard-Desce, M.; Mongin, O. *Synthesis* **2005**, *11*, 1771.
- (38) Shao, H.; Chen, X.; Wang, Z.; Lu, P. *J. Lumin.* **2007**, *127*, 349–354.
- (39) Kung, H. F.; Kung, M.-P.; Zhuang, Z.-P. U.S. Patent 7,297,820, 2007.
- (40) Hagiwara, T.; Sugiyama, H.; Matsushima, Y.; Kobyashi, T. U.S. Patent 5,573,878, 1996.
- (41) Xia, H. J.; He, J. T.; Peng, P.; Zhou, Y. H.; Li, Y. W.; Tian, W. *J. Tetrahedron Lett.* **2007**, *48*, 5877–5881.
- (42) Yang, Z.; Xu, B.; He, J.; Xue, L.; Guo, Q.; Xia, H.; Tian, W. *Org. Electron.* **2009**, *10*, 954–959.
- (43) Creason, S. C.; Wheeler, J.; Nelson, R. F. *J. Org. Chem.* **1972**, *37*, 4440–4446.
- (44) Iwan, A.; Sek, D. *Prog. Polym. Sci. (Oxford)* **2011**, *36*, 1277–1325.
- (45) Otero, L.; Sereno, L.; Fungo, F.; Liao, Y.-L.; Lin, C.-Y.; Wong, K.-T. *Chem. Mater.* **2006**, *18*, 3495–3502.
- (46) Zabel, P.; Dittrich, T.; Liao, Y.-I.; Lin, C.-Y.; Wong, K.-T.; Fernandez, L.; Fungo, F.; Otero, L. *Org. Electron.* **2009**, *10*, 1307–1313.
- (47) Natera, J.; Otero, L.; Sereno, L.; Fungo, F.; Wang, N.-S.; Tsai, Y.-M.; Hwu, T.-Y.; Wong, K.-T. *Macromolecules* **2007**, *40*, 4456–4463.
- (48) Yurchenko, O.; Freytag, D.; zur Borg, L.; Zentel, R.; Heinze, J.; Ludwigs, S. *J. Phys. Chem. B* **2012**, *116*, 30–39.